Universiteit Leiden
The Netherlands

Chemical biology studies on retaining exo-β-glucosidases

Su, Q.

Citation
Su, Q. (2024, November 6). *Chemical biology studies on retaining exo-β-glucosidases*. Retrieved from https://hdl.handle.net/1887/4107652

Version:	Publisher's Version
License:	Licence agreement concerning inclusion of doctoral thesis in the Institutional Repository of the University of Leiden
Downloaded from:	https://hdl.handle.net/1887/4107652

Note: To cite this publication please use the final published version (if applicable).

Chapter 4

Reactivity of cytosolic retaining β-glucosidase towards retaining glycosidase ABPs

Qin Su, Mats Bulterman, Maria Ferraz, Max Janssen, Rita Petracca, Marta Artola, Rolf G. Boot, Herman S. Overkleeft, and Johannes M. F. G. Aerts are acknowledged for their contributions to this chapter.

Abstract

The cytosolic glucosidase GBA3 (EC 3.2.1.21, CAZy GH1) is an enzyme with broad substrate specificity in mammals, where it is thought to partake in the degradation of glycosylated xenobiotics. In humans, inherited deficiency of GBA3 is relatively common but appears not to be accompanied by clinical manifestations. GBA3 is reported to hydrolyze a variety of glycosidic substrates, as is confirmed in this chapter for 4-methylumbelliferyl (4-MU)-β-D-glucopyranoside, 4-MU-β-D-galactopyranoside, 4-MU-β-D-fucopyranoside, 4-MU-β-D-xylopyranoside, and 4-MU-α-L-arabinopyranoside. Moreover, β-D-galactose-configured and α-L-arabinopyranose-configured cyclophellitol-aziridine ABPs were identified that label GBA3 with some selectivity over the other two human retaining glucosidases, GBA1 and GBA2.

Introduction

The cytosolic β-glucosidase, GBA3, also referred to as non-specific β-glucosidase, broad-specificity β-glycosidase, cytosolic β-glucosidase-like protein-1 (cBGL1), and Klotho related protein (KLrP), is a 469 amino acid cytosolic retaining β-exoglucosidase.[1-6] The human *GBA3* gene is located in locus 4p15.2, and GBA3 is expressed as a cytosolic protein in the liver, kidneys, and intestine, amongst other tissues.[5] GBA3 (EC 3.2.1.21) is classified as a member of family GH1 of retaining β-glycosidases in the CAZy database (www.cazy.org). The crystal structure of GBA3 reveals structural features of its catalytic pocket.[5,7,8] GBA3 employs a catalytic nucleophile (E373) and acid/base (E165) in β-glucoside hydrolysis.[5,7] GBA3 was found to hydrolyze many xenobiotic glycosides including dietary flavonoids and isoflavones and was therefore considered to play a role in xenobiotic metabolism.[3,9] In addition, it has been reported that GBA3 stabilizes NEU2 (sialidase-2, a cytosolic sialidase), and has a possible role in the catabolism of cytosolic sialic acid-free N-glycans.[10] Besides GBA3, human tissue express two other retaining β-glucosidases, namely, lysosomal GBA1 (EC 3.2.1.45, GH30) and cytosol facing membrane-bound GBA2 (EC 3.2.1.45, GH116).[7,11,12] Deficiency of GBA1 is at the basis of Gaucher disease (GD), a lysosomal storage disorder characterized by massive accumulation of glucosylceramide (GlcCer) in lysosomes of tissue macrophages.[13] Patients with the most common GD variant (type 1) do not develop neuropathological complaints, while patients suffering from the rarer variants of GD (type 2 and type 3) eventually develop potentially fatal CNS symptoms.[14] Deficiency of GBA2 in turn is associated with hereditary spastic paraplegia.[14] Dekker *et al.* reported that a common loss-of-function mutation in GBA3 does not correlate with type 1 GD severity.[15] This study corroborates earlier work by Beutler and colleagues, who did not observe a relationship between any of four GBA3 gene polymorphisms with GD manifestation severity.[16] The physiological role of GBA3 remains therefore enigmatic.

GBA3 differs from the other two cellular β-glucosidases (GBA1 and GBA2) in that it has a broad substrate specificity, in particular with respect to the nature of the monosaccharide in its substrate glycosides. GBA3 hydrolyzes, besides β-D-glucopyranosides, also β-D-galactopyranosides (β-D-Gal), β-D-fucopyranosides (β-D-Fuc), β-D-xylopyranosides (β-D-Xyl), and α-L-arabinosides.[1,2] Besides substrate hydrolysis, GBA3 has also been shown to have transglycosylase activity, producing β-xylosyl-cholesterol (XylChol) from both xylosylceramide and 4-MU-β-D-xylopyranoside as sugar donor and cholesterol as acceptor.[17] Transglycosylation activity is also a feature of GBA1 and GBA2, which transfer β-glucopyranose or β-galactopyranose from GlcCer or GalCer to cholesterol to produce β-glucosyl-cholesterol (GlcChol) or β-galactosyl-cholesterol (GalChol), respectively.[18,19] GBA3 however, while capable of producing XylChol, does not produce GlcChol, as GBA1 and GBA2 do.[17]

The studies described in this chapter were aimed to discover new tools to study GBA3 activity in complex biological milieu. For this purpose, recombinant GBA3 was exposed to a variety of fluorogenic substrates as well as cyclophellitol-based activity-based probes (ABPs) of various nature (configuration, substitution pattern). These studies identify that 4-MU-β-D-Fuc and 4-MU-α-L-Ara*p* are both efficiently and with reasonable selectivity processed by GBA3, and reveal that β-D-galactose configured (β-D-Gal) cyclophellitol ABP **3** and α-L-arabinopyranose configured (α-L-Ara*p*) cyclophellitol aziridine ABP **5** (Figure 1) label GBA3 with some selectivity over GBA1 and GBA2.

Results

Identification of a GBA3-selective fluorogenic substrate

The first research objective comprised the identification of a reporter substrate for monitoring the activity of GBA3 in biological samples. To this end, the ability of isolated recombinant human GBA3 (rhGBA3) to hydrolyze fifteen 4-methylumbelliferyl (4-MU)-glycosides was investigated first. Corroborating literature studies,[1,2] rhGBA3 efficiently hydrolyzes 4-MU-β-D-glucopyranoside (β-D-Glc), 4-MU-β-D-galactopyranoside (β-D-Gal), 4-MU-β-D-fucopyranoside (β-D-Fuc), and 4-MU-α-L-arabinopyranoside (α-L-Ara*p*), and to a lesser extent also 4-MU-β-D-xylopyranoside (β-D-Xyl) and 4-MU-α-L-arabinofuranoside (α-L-Ara*f*), but none of the other nine 4-MU-glycosides (Table 1A, see Figure 1 for the structures of the 4-MU-glycosides used). Although their proficiency as reporter substrate

differs, all six GBA3-sensitive substrates can in principle be used to report on GBA3 activity, and the effect of potential inhibitors on this, in settings in which GBA3 is the only retaining β-glucosidase present. Human cells, and extracts thereof, however contain a multitude of glycosidases, including GBA1 and GBA2, and the galactosidases, GLB1 (β-galactosidases, EC 3.2.1.23) and GALC (galactosylceramidase, EC 3.2.1.46).

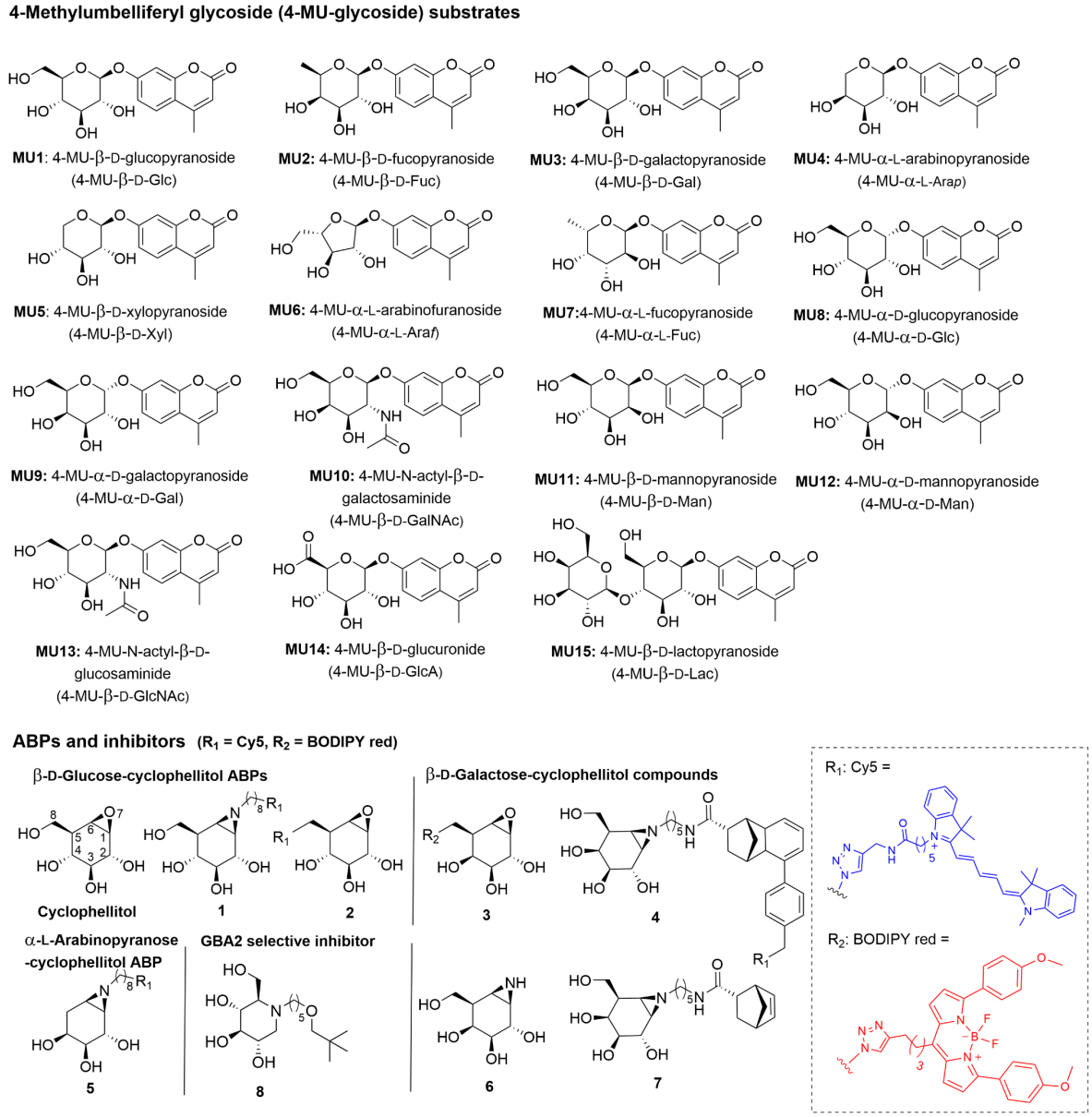

Figure 1. Chemical structure of compounds used in this chapter.

Substrates processed by one or more of these enzymes are not suitable for measuring specifically GBA3 activity in such more complex biological samples. For instance, 4-MU-β-D-Xyl is also hydrolyzed by GBA1, and 4-MU-β-D-Gal by GALC and GLB1. This does not necessarily hold true for 4-MU-β-D-Fuc, 4-MU-α-L-Ara*p*, and 4-MU-α-L-Ara*f*, as the ability of GBA1, GBA2, GALC and GLB1 to process these substrates is not known. To shed light in the possible use of 4-MU-β-D-Fuc, 4-MU-α-L-Ara*p*, or 4-MU-α-L-Ara*f* as selective GBA3 reporters, these three substrates were next exposed to either recombinant human (rh) GBA1 or lysates of GBA1/GBA2 KO HEK293T cells overexpressing GBA2 (hereafter termed GBA2 cells). As shown in Table 1B, neither 4-MU-β-D-Fuc nor 4-MU-α-L-Ara*p* proved to be rhGBA1 substrates, whereas some 4-MU-α-L-Ara*f* processing by rhGBA1 was observed. When exposed to GBA2 cell extract, 4-MU-β-D-Fuc and 4-MU-α-L-Ara*p* were processed with considerable efficiency, while no

discernible hydrolysis of 4-MU-α-L-Ara*f* was observed. GBA2 cell extract-mediated hydrolysis of 4-MU-β-D-Fuc and 4-MU-α-L-Ara*p* could be reduced largely by pretreatment with the potent GLB1 and GALC inhibitor,[20] *galacto*-cyclophellitol-aziridine **6**. In contrast, the potent and selective GBA2 inhibitor **8**[21] had no effect on the GBA2 cell extract-mediated hydrolysis of 4-MU-β-D-Fuc and 4-MU-α-L-Ara*p*. Taken these results together, 4-MU-β-D-Fuc and 4-MU-α-L-Ara*p* emerge as the most GBA3-selective substrates of the series tested and may be useful to report on GBA3 activity in mammalian cell extracts, provided that samples are pretreated with the GLB1/GALC inhibitor **6**.

Table 1. (A) Isolated rhGBA3 hydrolyzes six 4-MU-glycosides. 4-MU-glycosides (2-3.7 mM) in McIlvaine buffer (150 mM, pH 6.0) were incubated with rhGBA3 for 1 h at 37 °C (see Figure 1 for the structures of the fluorogenic substrates). (B) Processing of substrates by recombinant human GBA1 (rhGBA1), lysate of GBA1/GBA2 KO HEK293T cell, and lysate of GBA2 cells. Isolated rhGBA1 was incubated with the indicated substrate for 30 min at 37 °C at pH 5.2. Samples (lysates of either GBA1/GBA2 KO cells or GBA2 cells) were pre-incubated with vehicle (DMSO) or 500 nM inhibitor **6** (to selectively inhibit GLB1/GALC) or 500 nM inhibitor **8** (to selectively inhibit GBA2) for 30 min at 37 °C at pH 5.8, followed by incubation with indicated substrates for 30 min.

A			**B**				
4-MU-glycosides (2-3.7 mM, at pH 6.0)		**rhGBA3 activity** (μmol/h/mg)	**Activity**		**4-MU-β-D-Fuc (MU2)**	**4-MU-α-L-Ara*p* (MU4)**	**4-MU-α-L-Ara*f* (MU6)**
MU1	(β-D-Glc)	1441.7 ± 110.5	Isolated rhGBA1 (μmol/h/mg)		<1	<1	3.6
MU2	(β-D-Fuc)	1353.4 ± 14.7					
MU3	(β-D-Gal)	700.3 ± 19.5	Lysate of GBA1/ GBA2 KO cells (nmol/ h/mg)	No inhibitor (vehicle)	27.0	23.1	< 0.1
MU4	(α-L-Ara*p*)	300.9 ± 106.4					
MU5	(β-D-Xyl)	45.7 ± 15.9		+ GLB1/GALC selective inhibitor **6**	0.1	0.4	/
MU6	(α-L-Ara*f*)	14.6 ± 0.8					
MU7	(α-L-Fuc)	<1	Lysate of GBA2 cells (nmol/ h/mg)	No inhibitor (vehicle)	21.4	18.1	0.3
MU8	(α-D-Glc)	<1					
MU9	(α-D-Gal)	<1					
MU10	(β-D-GalNAc)	<1		+ GBA2 selective inhibitor **8**	20.5	17.3	/
MU11	(β-D-Man)	<1					
MU12	(α-D-Man)	<1					
MU13	(β-D-GlcNAc)	<1		+ GLB1/GALC selective inhibitor **6**	< 0.1	0.3	/
MU14	(β-D-GlcA)	<1					
MU15	(β-D-Lac)	<1					

Towards GBA3-selective activity-based probes

Activity-based protein profiling (ABPP) reports on active enzymes in a manner complementary to that of fluorogenic substrates. Whereas fluorogenic substrates are ideally suited for determining enzyme activity kinetics and enzyme inhibition constants, ABPP is particularly suited to detect and quantify enzymes in complex biological samples. With the aim to uncover a GBA3-selective ABP, lysates of HEK293T cells containing GBA1, GBA2, and GBA3 were incubated with ABPs **3**-**5**. These three ABPs were selected because they emulate in structure (configuration and substitution pattern) that of the most GBA3-reactive fluorogenic substrates identified in Table 1A, namely β-D-galactopyranoside (for **3** and **4**) and α-L-arabinofuranoside (for **5**). As shown in Figure 2A, β-D-*Gal*-cyclophellitol (β-D-Gal) ABP **3** gave selective GBA3 labelling above 3 µM without labelling GBA1 and GBA2. ABP **3** has been reported earlier to selectively label GALC,[22] which is however present in low amounts in the HEK293T cells used here,[22] and no clear GALC labelling of ABP **3** was observed under these conditions. β-D-*Gal*-cyclophellitol aziridine ABP **4** at or above 100 nM labels GBA3, but at these concentrations also labels GLB1. ABP **4** is reported[20] to react with GBA1 and GBA2, besides the galactosidases, GALC and GLB1, and labelling of GBA2 and GLB1 was observed here as well when treating HEK293T lysate with ABP **4**. α-L-Ara*p*-cyclophellitol (α-L-Ara*p*) aziridine ABP **5** labelled all three retaining β-glucosidases as well as GLB1 with some selectivity for GBA3 over GBA1 and GBA2. To investigate the reactivity of ABP **3** towards GBA1, mixtures of rhGBA1 and rhGBA3 were incubated with ABP **3**. As shown in Figure 2B, ABP **3** clearly labelled rhGBA3, but did not label rhGBA1. ABPs **3** and **5**, exhibiting relatively good selectivity towards GBA3 in ABPP assays, were then measured for their inhibitory potency (apparent IC_{50} values) towards retaining β-glucosidases in a 4-MU-β-D-Glc fluorogenic substrate assay. Both compounds proved to be somewhat rhGBA3-selective also in these assays.

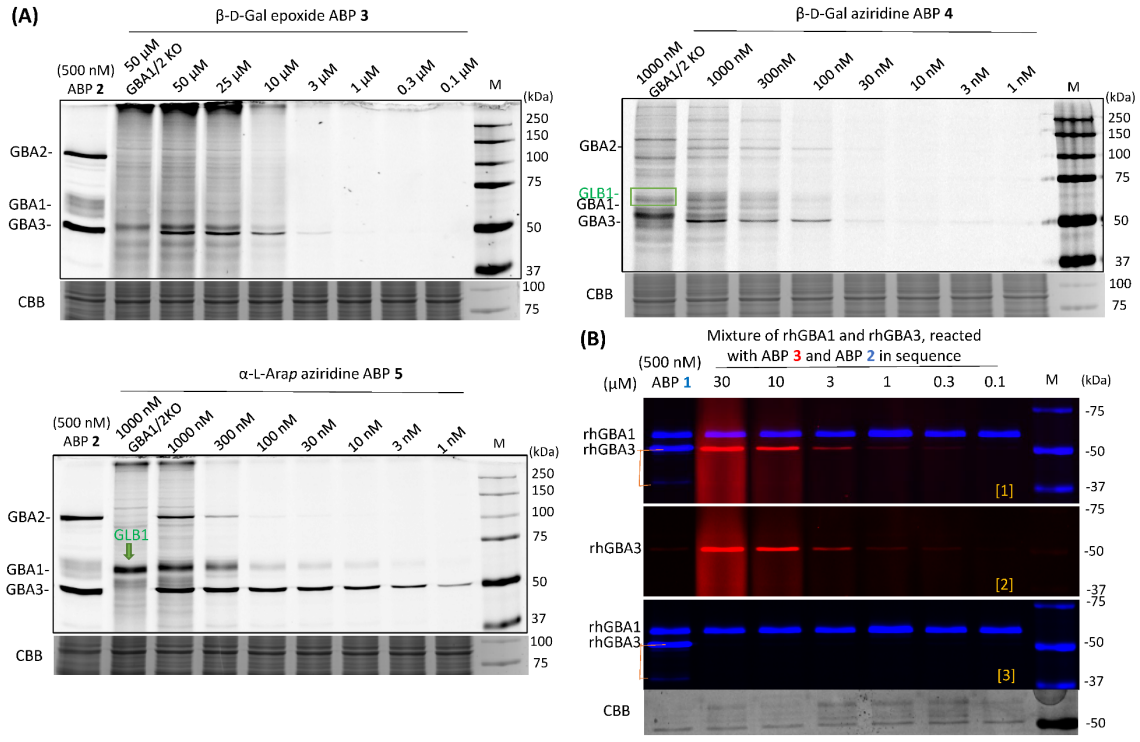

Figure 2. (A) Lysates of HEK293T cells expressing endogenous GBA1 and overexpressed GBA2 and GBA3, or of GBA1/GBA2 knockout (KO) HEK293T cells, were incubated with varying concentrations of ABPs (**3**-**5**) for 30 min at 37 °C, prior to SDS PAGE and fluorescence scanning of the wet gel slabs. (B) Mixtures of rhGBA1 and rhGBA3 were first treated with varying concentrations of ABP **3** for 30 min at 37 °C. Subsequently, samples were incubated with 250 nM GBA1 selective ABP **2** to show residual active rhGBA1. Labelling of 500 nM broad-spectrum β-glucosidase ABP **1** shows the presence of both rhGBA1 and rhGBA3. [1] Merged fluorescence of ABP **3** (shown as red) and ABP **1**, **2** (shown as blue). [2] Labelling of ABP **3** (red). [3] Labelling of ABP **1** and **2** (blue).

Table 2. Apparent IC_{50} of ABPs **3** and **5** towards GBA1, GBA2 and GBA3 as determined in a 4-MU-β-D-Glc fluorogenic substrate assay. Error ranges = ± SD, n= 2 replicates.

Apparent IC_{50} (nM) of	rhGBA1[a]	GBA2[b]	rhGBA3[c]
β-D-Gal epoxide **3**	> 100000	> 100000	1649.0 ± 145.7
α-L-Ara*p* aziridine **5**	433.8 ± 11.2	> 10000 [d]	1.60 ± 0.04

[a]rhGBA1 = Imiglucerase, isolated recombinant human GBA1. [b]GBA2 = lysate of GBA2 cells. [c] hGBA3 = isolated recombinant GBA3. The above enzymes were incubated with **3** or **5** for 30 min, following by incubation with 4-MU-β-D-Glc for 30 min. [d]GLB1/GALC in lysates were not inactivated. Error ranges = ± SD, n = 2 (duplicates).

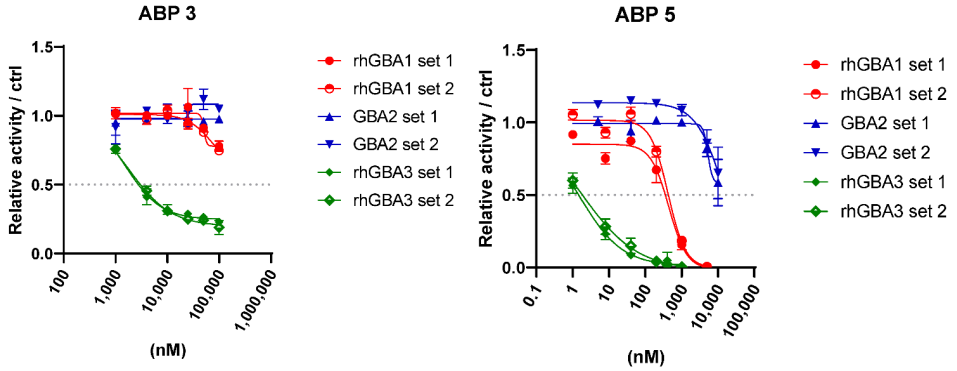

Figure 3. Apparent IC_{50} curve of ABP **3** and **5** as β-glucosidase inhibitors as measured in a 4-MU-β-D-Glc fluorogenic substrate assay.

Next, ABPs **3** and **5** were further examined on their selectivity towards β-glucosidases *in situ* (Figure 4). Intact HEK293T cells endogenously expressing GBA1 and overexpressing GBA2 and GBA3 were treated with varying concentrations of ABP **3** or **5** for 3 h *in situ.* The cells were then harvested and lysed, followed by the ABPP. ABP **3** labelled GBA3 without labelling GBA1 and GBA2, consistent with the *in vitro* ABPP assays. ABP **5** in contrast labelled all β-glucosidases at close concentration with concurrent GLB1 labelling, thus presenting no distinct GBA3 selectivity window *in situ*.

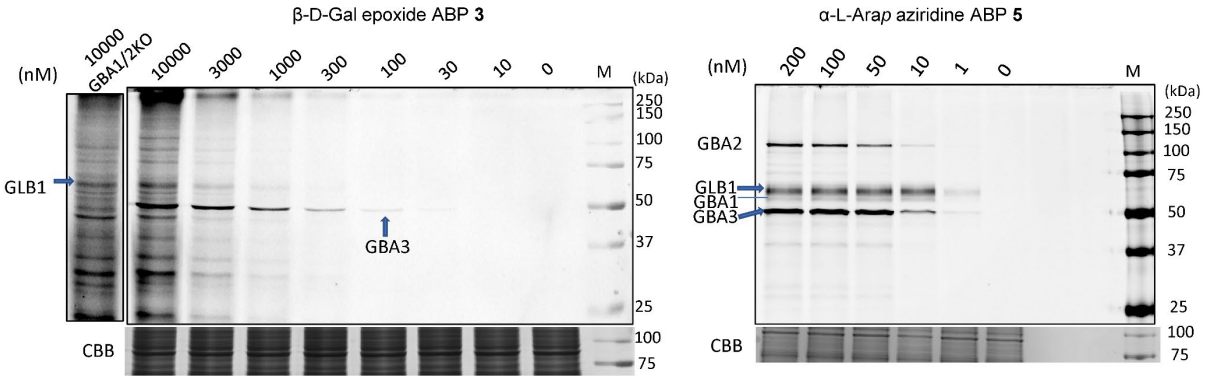

Figure 4. Intact HEK293T cells expressing endogenous GBA1 and overexpressing GBA2 and GBA3 were treated with varying concentrations of ABP **3** or **5** *in situ* for 3 h at 37 °C, then lysed, subjected to SDS-PAGE and fluorescence scanning of the wet gel slabs. As a background control intact GBA1/GBA2 KO HEK293T cells were also treated with ABP **3** at the same conditions.

Investigating the reactivity of β-D-Gal epoxide ABP 3 and α-L-Ara*p* aziridine ABP 5 with catalytic residue mutants of GBA3

It was previously demonstrated by site-directed mutagenesis that GBA3 reacts with the β-*Glc*-cyclophellitol aziridine ABP equipped with a BODIPY fluorophore through covalent linkage to the catalytic nucleophile (E373).[11] To establish whether ABPs **3** and **5** react GBA3 via the same catalytic residue, these two ABPs were incubated with either wild-type GBA3, the nucleophile mutant (E373G), the acid/base mutant (E165G), or the double mutant (E373G/E165G). Both probes reacted with the wild-type enzyme, whereas neither reacted with the nucleophile (E373G) and double (E165G/E373G) GBA3 mutants (Figure 5). Of note, the acid/base (E165G) mutant did react with ABP **5** but much less so with ABP **3**. As well, and in line with the results above, labelling of GLB1 with ABP **5** but not with **3** was observed.

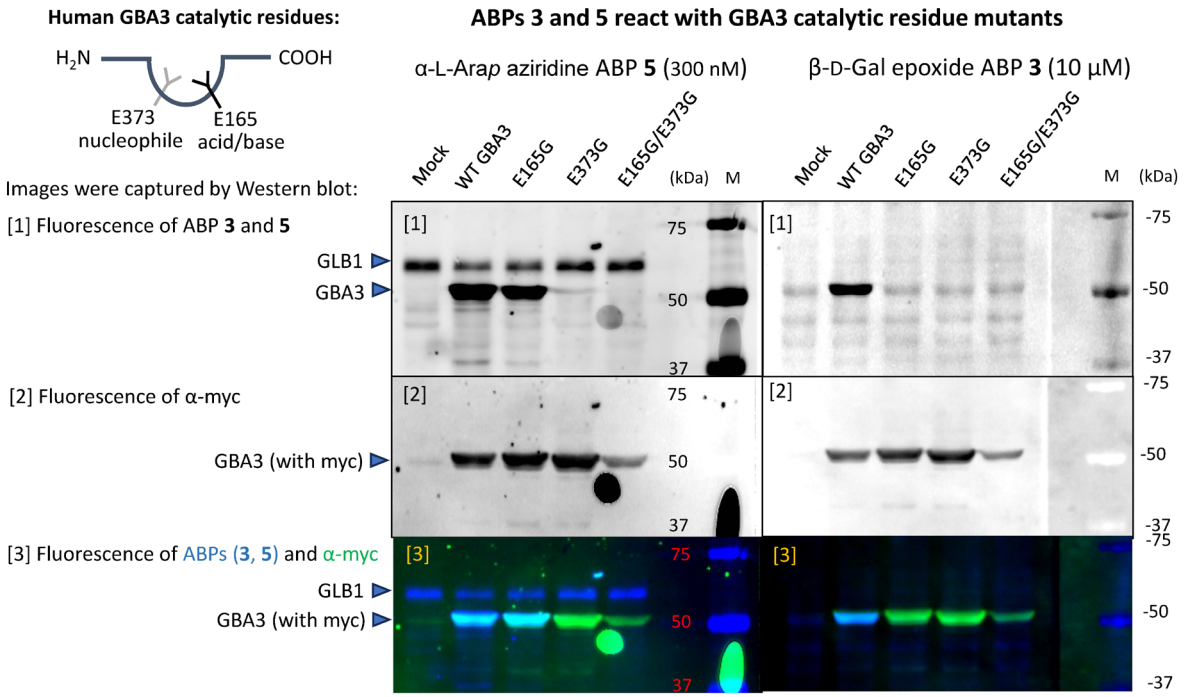

Figure 5. Reactivity of ABPs **3** and **5** towards wild-type GBA3 and GBA3 catalytic residue mutants (all enzymes used contain a myc tag). Lysates of GBA1/GBA2 KO HEK293T cells expressing either wild-type GBA3, or mutant GBA3 were incubated with ABP **3** or **5** for 30 min at 37 °C. After separating proteins with SDS-PAGE, proteins in the wet gel slabs were transferred to a nitrocellulose membrane. The nitrocellulose membrane was then subjected to anti-myc Western blotting. [1] Scanning fluorescence of Cy5 reporter of ABP **3** and **5**. [2] Scanning fluorescence of anti-myc (α-myc) antibody with Alexa Fluor™ 488 conjugation. [3] Merged fluorescence of both ABP **3**, **5** (blue) and anti-myc (green).

Discussion

The cytosolic β-glucosidase GBA3 was already identified in the early 1980s, but its physiological role remains elusive. Arguably, the lack of understanding on GBA3 is in part rooted in the scarcity of suitable reagents: fluorogenic substrates and activity-based probes able to selectively report on GBA3 activity. Indeed, such reagents have helped unraveling the role and activities of the two human retaining glucosidases most closely related to GBA3: GBA1 and GBA2 (see also Chapters 2 and 3). With this reasoning in mind, research was executed, as detailed in this chapter, aimed at identifying both a GBA3 selective fluorogenic substrate and an activity-based probe. From a panel of fifteen differently configured 4-MU-glycoside substrates, 4-MU-β-D-Fuc and 4-MU-α-L-Ara*p* were found as potentially suitable GBA3 selective substrates that can be used in mammalian cell extracts. When the retaining β-galactosidases, GALC and GLB1 (both of process 4-MU-β-D-Gal efficiently), are inactivated by the β-

galactosidase-selective inhibitor **6**, hydrolysis of 4-MU-β-D-Fuc and 4-MU-α-L-Ara*p* in human cell extracts can only be mediated by GBA3 and therefore selectively reflects the activity of GBA3. In the next set of experiments and based on the configurations identified in the fluorogenic substrate assays as accepted by GBA3, ABPs **3**-**5** were examined on their GBA3-reactivity and selectivity. Despite concurrent β-galactosidase (GLB1/GALC) labelling, both β-D-Gal epoxide ABP **3** and α-L-Ara*p* aziridine ABP **5** labelled GBA3 with relatively good selectivity over GBA1 and GBA2 *in vitro*. When intact HEK293T cells containing all cellular β-glucosidases were treated with ABP **3** or ABP **5** *in situ*, it was observed that ABP **5** did not maintain its GBA3 selectivity it exerts *in vitro*, while ABP **3** did. As well, the lack of reactivity of ABP **3** and **5** towards GBA3 catalytic nucleophile mutants supports the notion that both ABPs **3** and **5** react with GBA3 in an activity-based manner, forming a covalent and irreversible linkage with the GBA3 catalytic nucleophile (E373). Altogether, the results described in this chapter may help in unraveling the role of GBA3 in biology, by offering GBA3 reactive fluorogenic substrates and activity-based probes for detecting GBA3.

Experimental procedures

Materials

Imiglucerase (Cerezyme®), the isolated recombinant human GBA1 (rhGBA1), was kindly provided by Genzyme (Genzyme Nederland, Naarden, The Netherlands). Isolated recombinant human GBA3 (rhGBA3) was purchased from Bio-Techne R&D Systems (Catalog#: 5969-GH-010). 4-Methylumbelliferyl-glycoside substrates were bought from Glycosynth™ (UK), Sigma-Aldrich, or Biosynth Carbosynth. 4-Methylumbelliferone fluorescence was measured with a fluorimeter LS55 (Perkin Elmer, Waltham, MA, USA) with λ_{EX} 366 nm and λ_{EM} 445 nm. Polytron PT 1300D sonicator (Kinematica, Luzern, Switzerland) and potassium phosphate buffer (25 mM KH_2PO_4-K_2HPO_4, pH 6.5, supplemented with protease inhibitor cocktail (EDTA-free, Roche, Basel, Switzerland) and 0.1% (v/v) Triton X-100) were used for cell lysis. Protein concentrations were measured using Pierce BCA assay kit (Thermo Fisher Scientific, Waltham, MA, USA). Harvested cells (cell pellets) and cell lysates not used directly were stored at -80 °C. Wet gel slabs for ABPP and nitrocellulose membrane for Western blotting were imaged using a Typhoon FLA 9500 scanner (GE Healthcare) at λ_{EX} 532 nm and $\lambda_{EM} \geq$ 575 nm for the BODIPY red fluorescence and at λ_{EX} 635 nm and $\lambda_{EM} \geq$ 665 nm for Cy5 fluorescence. SDS-PAGE gels were stained for loading control of proteins with Coomassie G250 and scanned on a ChemiDoc MP imager (Bio-Rad, Hercules, CA, USA). The syntheses of the chemical compounds used in this study were previously reported in: **1**[23], **2**[24], **3** and **9**,[22] **4**, **6**, **7**,[20] and **8**.[21] Compound **5** was synthesized as described in the appendix. Cell lines of GBA1/GBA2 KO HEK293T, GBA1/GBA2 KO HEK293T with GBA2 OE (GBA2 cells), and HEK293T expressing endogenous GBA1 and overexpressed GBA2 and GBA3, were generated as described in Chapter 2.[25] Culture and lysis of HEK293T cells was conducted as described in Chapter 2.

4-MU-glycoside fluorogenic substrate assays for enzyme activity and apparent IC_{50} determination

4-MU-glycoside fluorogenic substrate assays for enzyme activity and apparent IC_{50} determination were conducted as described in Chapter 2 with the exception that isolated rhGBA3 was used instead of GBA3 in GBA1/GBA2 KO cell lysate for GBA3 activity measurement. For this, rhGBA3 was diluted in McIlvaine buffer (150 mM, pH 6.0, supplemented with 0.1% bovine serum albumin (BSA)) and was incubated with 2-3.7 mM of the indicated 4-MU-glycoside substrates dissolved in McIlvaine buffer (150 mM, pH 6.0, 0.1% (w/v) BSA) for 1 h at 37 °C.

In vitro ABPP

ABPP experiments were conducted as described in Chapter 2. In brief, samples containing GBA1, GBA2 or GBA3 (see for the exact constitution of these samples below) were incubated with the ABPs for 30 min (if not otherwise stated) at optimized conditions, followed by protein denaturing, SDS-PAGE and fluorescence scanning of the wet gel slabs. The incubation conditions for each enzyme were as follows: isolated rhGBA1 was incubated with the ABPs in McIlvaine buffer (150 mM, pH 5.2) supplemented with 0.1% (v/v) Triton X-100 and 0.2% (w/v) sodium taurocholate. Isolated rhGBA3 was incubated with the ABPs in McIlvaine buffer (150 mM, pH 6.0). In the case of incubating rhGBA3 with ABP for 1-3 h, 0.1% (w/v) BSA was added to the McIlvaine buffer. Lysates of HEK293T containing GBA1, GBA2 and GBA3, as well as GBA1/GBA2 KO HEK293T lysates were incubated with the ABPs in McIlvaine buffer (150 mM, pH 6.0).

In situ ABPP

Confluent GBA1/GBA2 KO HEK293T cells, or HEK293T cells expressing human endogenous GBA1 and overexpressing GBA2/GBA3, were cultured in 12-well dishes with (or without) the indicated ABPs for 3 h at 37 °C under 7% CO_2 atmosphere. After the incubation, cells were harvested and lysed as described in Chapter 2. After determination of the protein concentration by BCA assay, the lysates were adjusted to 10 µL by adding potassium phosphate buffer in order to normalize the amount of proteins

(10-25 µg total protein), after which the samples were subjected to SDS PAGE and in-gel fluorescence scanning.

GBA3 catalytic mutant labelling

For overexpression of GBA3 mutants, GBA1/GBA2 KO HEK293T were used for transfection. Wild-type GBA3, GBA3-E165G, GBA3-E373G, or GBA3- E165G/ E373G double mutants (all containing a myc tag) were generated as described previously for COS-7 cells.[11] Extracts of these were then incubated with ABP **3** or **5** for 30 min at 37 °C, and the samples were then subjected to SDS-PAGE and in-gel fluorescence scanning. Subsequently, proteins in the wet slab gels were transferred to a nitrocellulose membrane for Western blotting. Mouse anti-myc (α-myc) primary antibody (Bioke) and a secondary antibody (donkey anti-mouse IgG with an Alexa 488 fluorescent group, Invitrogen) were used to visualize myc-tagged, GBA3 wild-type and GBA3 mutants.

References

1. R. H. Glew, S. P. Peters and A. R. Christopher, Isolation and characterization of beta-glucosidase from the cytosol of rat kidney cortex, *Biochim. Biophys. Acta.*, 1976, **422**, 179-199.
2. L. B. Daniels, P. J. Coyle, Y. B. Chiao, R. H. Glew and R. S. Labow, Purification and characterization of a cytosolic broad specificity beta-glucosidase from human liver, *J. Biol. Chem.*, 1981, **256**, 13004-13013.
3. V. Gopalan, A. Pastuszyn, W. R. Galey and R. H. Glew, Exolytic hydrolysis of toxic plant glucosides by guinea pig liver cytosolic beta-glucosidase, *J. Biol. Chem.*, 1992, **267**, 14027-14032.
4. K. Yahata, K. Mori, H. Arai, S. Koide, Y. Ogawa, M. Mukoyama, A. Sugawara, S. Ozaki, I. Tanaka, Y. Nabeshima and K. Nakao, Molecular cloning and expression of a novel klotho-related protein, *J. Mol. Med.*, 2000, **78**, 389-394.
5. Y. Hayashi, N. Okino, Y. Kakuta, T. Shikanai, M. Tani, H. Narimatsu and M. Ito, Klotho-related protein is a novel cytosolic neutral beta-glycosylceramidase, *J. Biol. Chem.*, 2007, **282**, 30889-30900.
6. Y. Hayashi and M. Ito, Klotho-related protein KLrP: structure and functions, *Vitam. Horm.*, 2016, **101**, 1-16.
7. S. Tribolo, J. G. Berrin, P. A. Kroon, M. Czjzek and N. Juge, The crystal structure of human cytosolic beta-glucosidase unravels the substrate aglycone specificity of a family 1 glycoside hydrolase, *J. Mol. Biol.*, 2007, **370**, 964-975.
8. F. Ben Bdira, M. Artola, H. S. Overkleeft, M. Ubbink and J. M. Aerts, Distinguishing the differences in beta-glycosylceramidase folds, dynamics, and actions informs therapeutic uses, *J. Lipid. Res.*, 2018, **59**, 2262-2276.
9. J. G. Berrin, W. R. McLauchlan, P. Needs, G. Williamson, A. Puigserver, P. A. Kroon and N. Juge, Functional expression of human liver cytosolic beta-glucosidase in Pichia pastoris. Insights into its role in the metabolism of dietary glucosides, *Eur. J. Biochem.*, 2002, **269**, 249-258.
10. L. Wang, J. Seino, H. Tomotake, Y. Funakoshi, H. Hirayama and T. Suzuki, Co-expression of NEU2 and GBA3 causes a drastic reduction in cytosolic sialyl free N-glycans in human MKN45 stomach cancer cells-evidence for the physical interaction of NEU2 and GBA3, *Biomolecules*, 2015, **5**, 1499-1514.
11. W. W. Kallemeijn, M. D. Witte, T. M. Voorn-Brouwer, M. T. Walvoort, K. Y. Li, J. D. Codée, G. A. van der Marel, R. G. Boot, H. S. Overkleeft and J. M. Aerts, A sensitive gel-based method combining distinct cyclophellitol-based probes for the identification of acid/base residues in human retaining beta-glucosidases, *J. Biol. Chem.*, 2014, **289**, 35351-35362.
12. C. L. Kuo, W. W. Kallemeijn, L. T. Lelieveld, M. Mirzaian, I. Zoutendijk, A. Vardi, A. H. Futerman, A. H. Meijer, H. P. Spaink, H. S. Overkleeft, J. M. Aerts and M. Artola, In vivo inactivation of glycosidases by conduritol B epoxide and cyclophellitol as revealed by activity-based protein profiling, *FEBS J.*, 2019, **286**, 584-600.
13. J. Stirnemann, N. Belmatoug, F. Camou, C. Serratrice, R. Froissart, C. Caillaud, T. Levade, L. Astudillo, J. Serratrice, A. Brassier, C. Rose, T. Billette de Villemeur and M. G. Berger, A review of Gaucher disease pathophysiology, clinical presentation and treatments, *Int. J. Mol. Sci.*, 2017, **18**, 441.
14. J. M. Aerts, C. L. Kuo, L. T. Lelieveld, D. E. C. Boer, M. J. C. van der Lienden, H. S. Overkleeft and M. Artola, Glycosphingolipids and lysosomal storage disorders as illustrated by Gaucher disease, *Curr. Opin. Chem. Biol.*, 2019, **53**, 204-215.
15. N. Dekker, T. Voorn-Brouwer, M. Verhoek, T. Wennekes, R. S. Narayan, D. Speijer, C. E. Hollak, H. S. Overkleeft, R. G. Boot and J. M. Aerts, The cytosolic beta-glucosidase GBA3 does not influence type 1 Gaucher disease manifestation, *Blood Cells Mol. Dis.*, 2011, **46**, 19-26.
16. E. Beutler, L. Beutler and C. West, Mutations in the gene encoding cytosolic beta-glucosidase in Gaucher disease, *J. Lab. Clin. Med.*, 2004, **144**, 65-68.
17. D. E. Boer, M. Mirzaian, M. J. Ferraz, K. C. Zwiers, M. V. Baks, M. D. Hazeu, R. Ottenhoff, A. R. A. Marques, R. Meijer, J. C. P. Roos, T. M. Cox, R. G. Boot, N. Pannu, H. S. Overkleeft, M. Artola and

J. M. Aerts, Human glucocerebrosidase mediates formation of xylosyl-cholesterol by beta-xylosidase and transxylosidase reactions, *J. Lipid. Res.*, 2021, **62**, 100018.

18. A. R. Marques, M. Mirzaian, H. Akiyama, P. Wisse, M. J. Ferraz, P. Gaspar, K. Ghauharali-van der Vlugt, R. Meijer, P. Giraldo, P. Alfonso, P. Irun, M. Dahl, S. Karlsson, E. V. Pavlova, T. M. Cox, S. Scheij, M. Verhoek, R. Ottenhoff, C. P. van Roomen, N. S. Pannu, M. van Eijk, N. Dekker, R. G. Boot, H. S. Overkleeft, E. Blommaart, Y. Hirabayashi and J. M. Aerts, Glucosylated cholesterol in mammalian cells and tissues: formation and degradation by multiple cellular beta-glucosidases, *J. Lipid. Res.*, 2016, **57**, 451-463.
19. H. Akiyama, M. Ide, Y. Nagatsuka, T. Sayano, E. Nakanishi, N. Uemura, K. Yuyama, Y. Yamaguchi, H. Kamiguchi, R. Takahashi, J. M. Aerts, P. Greimel and Y. Hirabayashi, Glucocerebrosidases catalyze a transgalactosylation reaction that yields a newly-identified brain sterol metabolite, galactosylated cholesterol, *J. Biol. Chem.*, 2020, **295**, 5257-5277.
20. C. L. Kuo, Q. Su, A. van den Nieuwendijk, T. J. M. Beenakker, W. A. Offen, L. I. Willems, R. G. Boot, A. J. Sarris, A. R. A. Marques, J. D. C. Codée, G. A. van der Marel, B. I. Florea, G. J. Davies, H. S. Overkleeft and J. M. Aerts, The development of a broad-spectrum retaining beta-exo-galactosidase activity-based probe, *Org. Biomol. Chem.*, 2023, **21**, 7813-7820.
21. D. Lahav, B. Liu, R. van den Berg, A. van den Nieuwendijk, T. Wennekes, A. T. Ghisaidoobe, I. Breen, M. J. Ferraz, C. L. Kuo, L. Wu, P. P. Geurink, H. Ovaa, G. A. van der Marel, M. van der Stelt, R. G. Boot, G. J. Davies, J. M. Aerts and H. S. Overkleeft, A Fluorescence Polarization Activity-Based Protein Profiling assay in the discovery of potent, selective inhibitors for human nonlysosomal glucosylceramidase, *J. Am. Chem. Soc.*, 2017, **139**, 14192-14197.
22. A. R. Marques, L. I. Willems, D. Herrera Moro, B. I. Florea, S. Scheij, R. Ottenhoff, C. P. van Roomen, M. Verhoek, J. K. Nelson, W. W. Kallemeijn, A. Biela-Banas, O. R. Martin, M. B. Cachon-Gonzalez, N. N. Kim, T. M. Cox, R. G. Boot, H. S. Overkleeft and J. M. Aerts, A specific activity-based probe to monitor family GH59 galactosylceramidase, the enzyme deficient in Krabbe disease, *ChemBioChem*, 2017, **18**, 402-412.
23. S. P. Schröder, J. W. van de Sande, W. W. Kallemeijn, C. L. Kuo, M. Artola, E. J. van Rooden, J. Jiang, T. J. M. Beenakker, B. I. Florea, W. A. Offen, G. J. Davies, A. J. Minnaard, J. M. Aerts, J. D. C. Codée, G. A. van der Marel and H. S. Overkleeft, Towards broad spectrum activity-based glycosidase probes: synthesis and evaluation of deoxygenated cyclophellitol aziridines, *Chem. Commun.*, 2017, **53**, 12528-12531.
24. M. Artola, C. L. Kuo, L. T. Lelieveld, R. J. Rowland, G. A. van der Marel, J. D. C. Codée, R. G. Boot, G. J. Davies, J. M. Aerts and H. S. Overkleeft, Functionalized cyclophellitols are selective glucocerebrosidase inhibitors and induce a bona fide neuropathic Gaucher model in zebrafish, *J. Am. Chem. Soc.*, 2019, **141**, 4214-4218.
25. Q. Su, S. P. Schröder, L. T. Lelieveld, M. J. Ferraz, M. Verhoek, R. G. Boot, H. S. Overkleeft, J. M. Aerts, M. Artola and C. L. Kuo, Xylose-configured cyclophellitols as selective inhibitors for glucocerebrosidase, *ChemBioChem*, 2021, **22**, 3090-3098.

Appendix

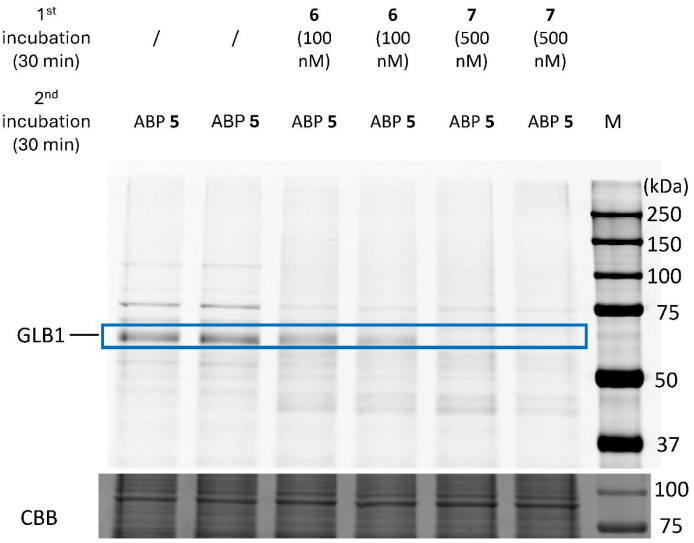

Figure S1. Reaction of α-L-Ara*p* aziridine ABP **5** towards GLB1 in cell lysate was inhibited by pre-treatment of GLB1/GALC selective inhibitor **6** or **7**. Lysates of GBA1/GBA2 KO HEK293T were treated with **6** (100 nM) or **7** (500 nM) for 30 min at 37 °C *in vitro*, followed by incubation with ABP **5** (200 nM) for 30 min, then samples were subjected to SDS-PAGE followed by in-gel fluorescence scanning.

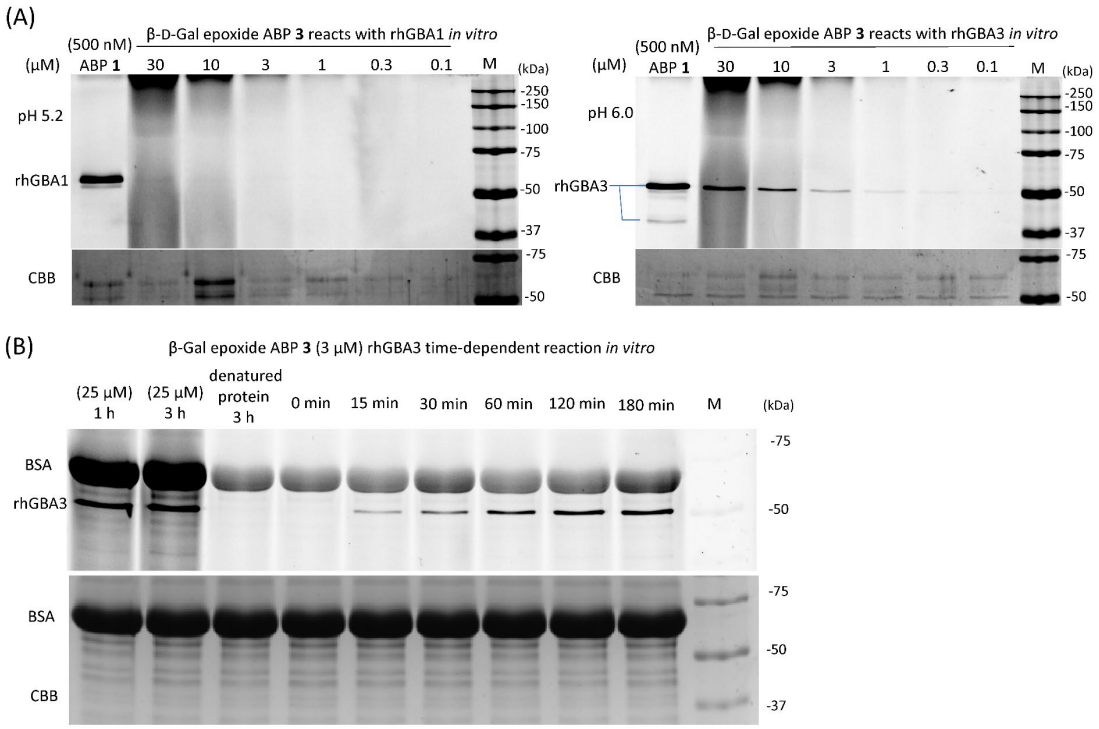

Figure S2. (A) Reactivity of β-D-Gal ABP **3** towards isolated rhGBA1 and rhGBA3 *in vitro*, isolated rhGBA1 or rhGBA3 was incubated with ABP **3** at the indicated pH for 30 min at 37 °C, then samples were subjected to SDS-PAGE and in-gel fluorescence scanning. (B) time-dependent interaction of ABP **3** towards rhGBA3, isolated rhGBA3 was incubated with ABP **3** at pH 6.0 at 37 °C for varying incubation times and subsequently subjected to SDS-PAGE and fluorescence scanning of the wet gel slabs. Bovine serum albumin (BSA) visible at around 65 kDa was added for stabilizing the isolated rhGBA3. Reactivity of ABP **3** towards denatured rhGBA3: rhGBA3 sample was first boiled at 98 °C for 5 min, followed by incubation with ABP **3** for 3 h at pH 6.

Table S1. Comparing hydrolysis activity of GBA1/GBA2 KO HEK293T cell lysates (containing GLB1 and GALC) towards 4-MU-β-D-Gal, 4-MU-β-D-Fuc and 4-MU-α-L-Ara*p*. Lysates were first incubated at 37 °C with or without 500 nM **6** (GALC/GLB1 inhibitor) for 30 min at pH 5 or pH 6, following incubation with indicated 4-MU-glycoside for 30 min. Hydrolysis activity of lysate towards these 4-MU-glycosides is shown as nmol per hour per mg (nmol/h/ng).

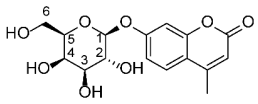

4-MU-β-D-Gal

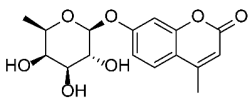

4-MU-β-D-Fuc

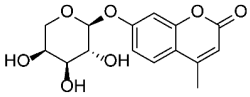

4-MU-α-L-Ara*p*

Activity (nmol/h/mg) of HEK239T GBA1/2 KO lysate				
Substrates	At pH 5.0		At pH 6.0	
	No inhibitor	+ GLB1/GALC inhibitor **6** (500 nM)	No inhibitor	+ GLB1/GALC inhibitor **6** (500 nM)
4-MU-β-D-Gal	222.2	0.9	71.8	< 0.1
4-MU-β-D-Fuc	23.5	< 0.1	8.2	< 0.1
4-MU-α-L-Ara*p*	17.0	< 0.1	4.6	< 0.1

Table S2. (A) Activity of β-D-galactose configured aziridine inhibitor (**6**, **7**), and β-D-galactose configured epoxide inhibitor **9** towards rhGBA3. (B) Activity of β-L-Ara*p* inhibitors (**10**, **11**)[1], α-L-Arap inhibitors (**12**, **13**)[1] towards β-glucosidases, examined by 4-MU-β-D-Glc fluorogenic substrate assays for 30 min incubation at 37 °C.

(A)

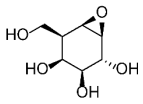

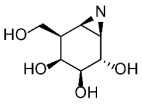

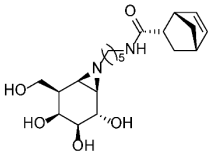

Remaining rhGBA3 activity (%)	β-D-Gal epoxide **9**	β-D-Gal aziridine **6**	β-D-Gal aziridine **7**
+ Inhibitor 10,000 nM	96%	30%	23%
+ Inhibitor 1,000 nM	97%	57%	50%
+ Inhibitor 100 nM	95%	83%	84%
+ Inhibitor 0 nM	100%	100%	100%

(B)

Remaining enzyme activity (%) with 50 µM inhibitors	**rhGBA1**	**GBA2**	**rhGBA3**
β-L-Ara*p* epoxide **10** 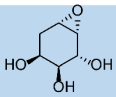	100%	100%	100%
β-L-Ara*p* aziridine **11** 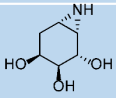	91%	100%	91%
α-L-Ara*p* epoxide **12** 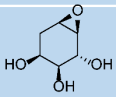	99%	100%	99%
α-L-Ara*p* aziridine **13** 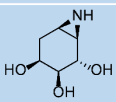	90%	97%	100%

Table S3. An overview of the reactivity of ABPs and inhibitors towards β-glucosidases and other glycosidases. '/' = no available data.

substrates	Inhibitors and ABPs	Apparent IC_{50} (nM)				Apparent IC_{50} values derived from
		GBA1	GBA2	GBA3	Other enzymes	
4-MU-β-D-Glc	β-D-*Glc*-cyclophellitol ABP **2**[2]	(1) 3.2 ± 0.17 ; (2) 45.20 ± 4.54	(1) 412,000 ± 10,100; (2) > 5000	(2) 5784 ± 79	/	(1) Ref[2]; (2) Ref[3]
	β-D-*Glc*-cyclophellitol aziridine ABP **1**[4]	8.10 ± 1.94	21.5 ± 0.42	8.54 ± 1.18	/	Ref[3]
4-MU-β-D-Fuc	Available ABP is not reported at present	/	/	/	/	/
4-MU-β-D-Gal	β-D-*Gal*-cyclophellitol ABP **3**[5]	> 1 x 10^5	> 1 x 10^5	1649.0 ± 145.7	GALC: 2800	Ref [5]
	β-D-*Gal*-cyclophellitol aziridine ABP **4**[6]	85.8	752	/	GLB1: 14.6 ± 0.98; GALC: 61.0 ± 6.89	
	β-D-*Gal*-cyclophellitol aziridine inhibitor **6**[6]	1560	3290	~ 1000	GLB1 : 2.55 ± 0.59; GALC: 5.57± 0.36	Ref [6]; Chapter 4
	β-D-*Gal*-cyclophellitol aziridine inhibitor **7**[6]	5370	> 10^4	~ 1000	GLB1 : 57.8 ± 3.05; GALC: 98.6 ± 20.8	
4-MU-α-L-Ara*p*	α-L-*Arap*-cyclophellitol aziridine ABP **5**	433.8 ± 11.2	> 10^4	1.60 ± 0.04	/	Chapter 4
4-MU-β-D-Xyl	β-D-*Xyl*-cyclophellitol aziridine ABP[3]	6.4 ± 0.5	544 ± 110	10,055 ± 1,003	/	Chapter 2
4-MU-α-L-Ara*f*	α-L-*Araf*-cyclophellitol aziridine ABP[7]	> 5 x 10^4	1,850	> 5 x 10^4	/	Chapter 3

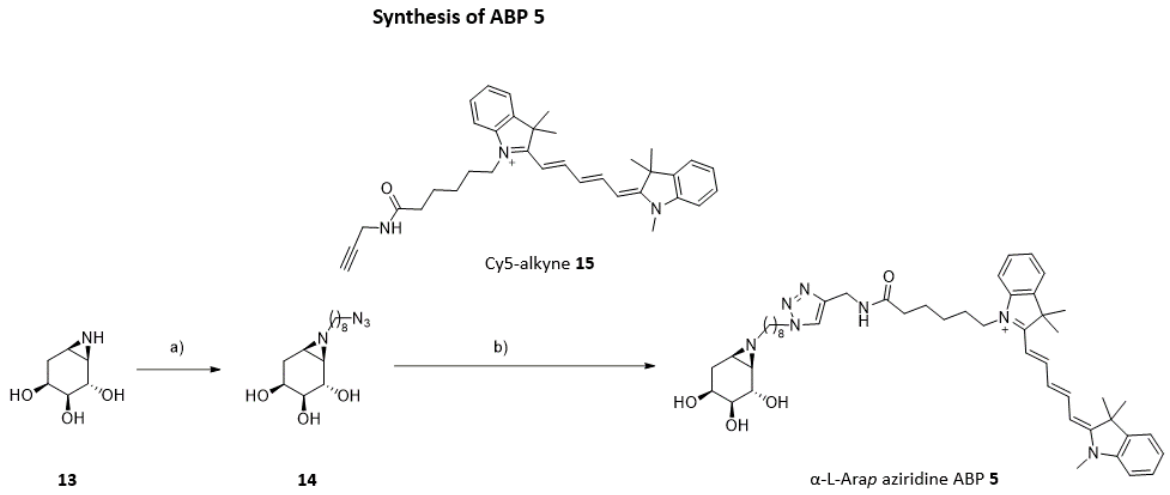

Scheme S1. Synthesis route of ABP **5**. Reagents and conditions: (a) 1-azido-8-iodo-octane, K_2CO_3, DMF, 60 °C. (b) $CuSO_4$, sodium ascorbate, Cy5-alkyne, DMF, rt.

To a solution of (1*R*,3*S*,4*S*,5*S*,6*R*)-7-azabicyclo[4.1.0]heptane-3,4,5-triol (**13**)[1] (0.010 g, 0.07 mmol) in dry DMF (3.0 mL), 1-azido-8-iodo-octane (0.039 g, 0.14 mmol) and K_2CO_3 (0.029 g, 0.21 mmol) were added. The reaction was left to stir at 60 °C under nitrogen atmosphere. After 15 hours, DMF was evaporated and the crude product purified by silica gel chromatography using a mixture of DCM/MeOH (from 100:0 to 90:10). The thus obtained product **14**, which was obtained together with minor impurities (0.008 g, 0.027 mmol) was dissolved in dry DMF (1.0 mL), to which a degassed solution of $CuSO_4{\cdot}5H_2O$ (40 mL, 0.018 mmol) and sodium ascorbate (0.004 g, 0.020 mmol) were added. After 10 min of stirring Cy5-alkyne **15** was added and the blue solution was stirred at room temperature for 15 hours. HPLC purification (C18 semipreparative column, solvent A: H_2O/NH_4OH, solvent B: CH_3CN) afforded compound **7** (0.009 g, 40%). ^{1}H NMR (400 MHz, $CDCl_3$): δ 8.24 (ddd, *J* = 14.5, 12.6, 2.7 Hz, 2H), 7.84 (s, 1H), 7.49 (dd, *J* = 7.5, 1.2 Hz, 2H), 7.41 (tdd, *J* = 7.4, 6.1, 1.2 Hz, 2H), 7.33 – 7.18 (m, 4H), 6.61 (t, *J* = 12.4 Hz, 1H), 6.34 – 6.16 (m, 2H), 4.40 (s, 2H), 4.36 (s, 2H), 4.08 (t, *J* = 7.6 Hz, 2H), 3.99 (d, *J* = 6.2 Hz, 1H), 3.73 (td, *J* = 2.3, 5.8 Hz, 1H), 3.62 (s, 4H), 3.34 (s, 4H), 2.32 – 2.17 (m, 4H), 2.05 – 1.99 (m, 2H), 1.90 – 1.84 (m, 6H), 1.84 – 1.76 (m, 2H), 1.72 (s, 17H), 1.53 – 1.42 (m, 4H), 1.41 – 1.21 (m, 13H) ppm. ^{13}C NMR (101 MHz, $CDCl_3$): δ176.6, 176.3, 175.5, 145.1, 144.4, 143.5, 143.4, 130.6, 130.6, 127.5, 127.1, 125.0, 124.3, 112.7, 105.1, 77.5, 71.8, 69.8, 61.2, 52.2, 45.1, 37.3, 36.4, 32.1, 29.1, 28.1, 28.6, 28.2, 28.2, 27.3 ppm.

Supplemental references

1. S. P. Schröder, R. Petracca, H. Minnee, M. Artola, J. M. Aerts, J. D. C. Codée, G. A. van der Marel and H. S. Overkleeft, A divergent synthesis of L-arabino- and D-xylo-configured cyclophellitol epoxides and aziridines, *Eur. J. Org. Chem.*, 2016, 4787-4794.
2. M. Artola, C. L. Kuo, L. T. Lelieveld, R. J. Rowland, G. A. van der Marel, J. D. C. Codée, R. G. Boot, G. J. Davies, J. M. Aerts and H. S. Overkleeft, Functionalized cyclophellitols are selective glucocerebrosidase inhibitors and induce a bona fide neuropathic Gaucher model in zebrafish, *J. Am. Chem. Soc.*, 2019, **141**, 4214-4218.
3. Q. Su, S. P. Schröder, L. T. Lelieveld, M. J. Ferraz, M. Verhoek, R. G. Boot, H. S. Overkleeft, J. M. Aerts, M. Artola and C. L. Kuo, Xylose-configured cyclophellitols as selective inhibitors for glucocerebrosidase, *ChemBioChem*, 2021, **22**, 3090-3098.
4. S. P. Schröder, J. W. van de Sande, W. W. Kallemeijn, C. L. Kuo, M. Artola, E. J. van Rooden, J. Jiang, T. J. M. Beenakker, B. I. Florea, W. A. Offen, G. J. Davies, A. J. Minnaard, J. M. Aerts, J. D. C. Codée, G. A. van der Marel and H. S. Overkleeft, Towards broad spectrum activity-based

glycosidase probes: synthesis and evaluation of deoxygenated cyclophellitol aziridines, *Chem. Commun.*, 2017, **53**, 12528-12531.

5. A. R. Marques, L. I. Willems, D. Herrera Moro, B. I. Florea, S. Scheij, R. Ottenhoff, C. P. van Roomen, M. Verhoek, J. K. Nelson, W. W. Kallemeijn, A. Biela-Banas, O. R. Martin, M. B. Cachon-Gonzalez, N. N. Kim, T. M. Cox, R. G. Boot, H. S. Overkleeft and J. M. Aerts, A specific activity-based probe to monitor family GH59 galactosylceramidase, the enzyme deficient in Krabbe disease, *ChemBioChem*, 2017, **18**, 402-412.
6. C. L. Kuo, Q. Su, A. van den Nieuwendijk, T. J. M. Beenakker, W. A. Offen, L. I. Willems, R. G. Boot, A. J. Sarris, A. R. A. Marques, J. D. C. Codée, G. A. van der Marel, B. I. Florea, G. J. Davies, H. S. Overkleeft and J. M. Aerts, The development of a broad-spectrum retaining beta-exo-galactosidase activity-based probe, *Org. Biomol. Chem.*, 2023, **21**, 7813-7820.
7. N. G. S. McGregor, M. Artola, A. Nin-Hill, D. Linzel, M. Haon, J. Reijngoud, A. Ram, M. N. Rosso, G. A. van der Marel, J. D. C. Codée, G. P. van Wezel, J. G. Berrin, C. Rovira, H. S. Overkleeft and G. J. Davies, Rational design of mechanism-based inhibitors and activity-based probes for the identification of retaining alpha-L-arabinofuranosidases, *J. Am. Chem. Soc.*, 2020, **142**, 4648-4662.